DØ Paper XXXX

The Ratio of Isolated Photon Cross Sections at $\sqrt{s} = 630$ GeV and 1800 GeV

V.M. Abazov,[23] B. Abbott,[58] A. Abdesselam,[11] M. Abolins,[51] V. Abramov,[26] B.S. Acharya,[17] D.L. Adams,[60] M. Adams,[38] S.N. Ahmed,[21] G.D. Alexeev,[23] G.A. Alves,[2] N. Amos,[50] E.W. Anderson,[43] M.M. Baarmand,[55] V.V. Babintsev,[26] L. Babukhadia,[55] T.C. Bacon,[28] A. Baden,[47] B. Baldin,[37] P.W. Balm,[20] S. Banerjee,[17] E. Barberis,[30] P. Baringer,[44] J. Barreto,[2] J.F. Bartlett,[37] U. Bassler,[12] D. Bauer,[28] A. Bean,[44] M. Begel,[54] A. Belyaev,[35] S.B. Beri,[15] G. Bernardi,[12] I. Bertram,[27] A. Besson,[9] R. Beuselinck,[28] V.A. Bezzubov,[26] P.C. Bhat,[37] V. Bhatnagar,[11] M. Bhattacharjee,[55] G. Blazey,[39] S. Blessing,[35] A. Boehnlein,[37] N.I. Bojko,[26] F. Borcherding,[37] K. Bos,[20] A. Brandt,[60] R. Breedon,[31] G. Briskin,[59] R. Brock,[51] G. Brooijmans,[37] A. Bross,[37] D. Buchholz,[40] M. Buehler,[38] V. Buescher,[14] V.S. Burtovoi,[26] J.M. Butler,[48] F. Canelli,[54] W. Carvalho,[3] D. Casey,[51] Z. Casilum,[55] H. Castilla-Valdez,[19] D. Chakraborty,[39] K.M. Chan,[54] S.V. Chekulaev,[26] D.K. Cho,[54] S. Choi,[34] S. Chopra,[56] J.H. Christenson,[37] M. Chung,[38] D. Claes,[52] A.R. Clark,[30] J. Cochran,[34] L. Coney,[42] B. Connolly,[35] W.E. Cooper,[37] D. Coppage,[44] M.A.C. Cummings,[39] D. Cutts,[59] G.A. Davis,[54] K. Davis,[29] K. De,[60] S.J. de Jong,[21] K. Del Signore,[50] M. Demarteau,[37] R. Demina,[45] P. Demine,[9] D. Denisov,[37] S.P. Denisov,[26] S. Desai,[55] H.T. Diehl,[37] M. Diesburg,[37] G. Di Loreto,[51] S. Doulas,[49] P. Draper,[60] Y. Ducros,[13] L.V. Dudko,[25] S. Duensing,[21] L. Duflot,[11] S.R. Dugad,[17] A. Duperrin,[10] A. Dyshkant,[26] D. Edmunds,[51] J. Ellison,[34] V.D. Elvira,[37] R. Engelmann,[55] S. Eno,[47] G. Eppley,[62] P. Ermolov,[25] O.V. Eroshin,[26] J. Estrada,[54] H. Evans,[53] V.N. Evdokimov,[26] T. Fahland,[33] S. Feher,[37] D. Fein,[29] T. Ferbel,[54] F. Filthaut,[21] H.E. Fisk,[37] Y. Fisyak,[56] E. Flattum,[37] F. Fleuret,[30] M. Fortner,[39] K.C. Frame,[51] S. Fu,[53] S. Fuess,[37] E. Gallas,[37] A.N. Galyaev,[26] M. Gao,[53] V. Gavrilov,[24] R.J. Genik II,[27] K. Genser,[37] C.E. Gerber,[38] Y. Gershtein,[59] R. Gilmartin,[35] G. Ginther,[54] B. Gómez,[5]

G. Gómez,[47] P.I. Goncharov,[26] J.L. González Solís,[19] H. Gordon,[56] L.T. Goss,[61] K. Gounder,[37] A. Goussiou,[28] N. Graf,[56] G. Graham,[47] P.D. Grannis,[55] J.A. Green,[43] H. Greenlee,[37] S. Grinstein,[1] L. Groer,[53] S. Grünendahl,[37] A. Gupta,[17] S.N. Gurzhiev,[26] G. Gutierrez,[37] P. Gutierrez,[58] N.J. Hadley,[47] H. Haggerty,[37] S. Hagopian,[35] V. Hagopian,[35] R.E. Hall,[32] P. Hanlet,[49] S. Hansen,[37] J.M. Hauptman,[43] C. Hays,[53] C. Hebert,[44] D. Hedin,[39] J.M. Heinmiller,[38] A.P. Heinson,[34] U. Heintz,[48] T. Heuring,[35] M.D. Hildreth,[42] R. Hirosky,[63] J.D. Hobbs,[55] B. Hoeneisen,[8] Y. Huang,[50] R. Illingworth,[28] A.S. Ito,[37] M. Jaffré,[11] S. Jain,[17] R. Jesik,[41] K. Johns,[29] M. Johnson,[37] A. Jonckheere,[37] M. Jones,[36] H. Jöstlein,[37] A. Juste,[37] S. Kahn,[56] E. Kajfasz,[10] A.M. Kalinin,[23] D. Karmanov,[25] D. Karmgard,[42] Z. Ke,[4] R. Kehoe,[51] A. Kharchilava,[42] S.K. Kim,[18] B. Klima,[37] B. Knuteson,[30] W. Ko,[31] J.M. Kohli,[15] A.V. Kostritskiy,[26] J. Kotcher,[56] B. Kothari,[53] A.V. Kotwal,[53] A.V. Kozelov,[26] E.A. Kozlovsky,[26] J. Krane,[43] M.R. Krishnaswamy,[17] P. Krivkova,[6] S. Krzywdzinski,[37] M. Kubantsev,[45] S. Kuleshov,[24] Y. Kulik,[55] S. Kunori,[47] A. Kupco,[7] V.E. Kuznetsov,[34] G. Landsberg,[59] W.M. Lee,[35] A. Leflat,[25] C. Leggett,[30] F. Lehner,[37] J. Li,[60] Q.Z. Li,[37] X. Li,[4] J.G.R. Lima,[3] D. Lincoln,[37] S.L. Linn,[35] J. Linnemann,[51] R. Lipton,[37] A. Lucotte,[9] L. Lueking,[37] C. Lundstedt,[52] C. Luo,[41] A.K.A. Maciel,[39] R.J. Madaras,[30] V.L. Malyshev,[23] V. Manankov,[25] H.S. Mao,[4] T. Marshall,[41] M.I. Martin,[37] R.D. Martin,[38] K.M. Mauritz,[43] B. May,[40] A.A. Mayorov,[41] R. McCarthy,[55] J. McDonald,[35] T. McMahon,[57] H.L. Melanson,[37] M. Merkin,[25] K.W. Merritt,[37] C. Miao,[59] H. Miettinen,[62] D. Mihalcea,[58] C.S. Mishra,[37] N. Mokhov,[37] N.K. Mondal,[17] H.E. Montgomery,[37] R.W. Moore,[51] M. Mostafa,[1] H. da Motta,[2] E. Nagy,[10] F. Nang,[29] M. Narain,[48] V.S. Narasimham,[17] H.A. Neal,[50] J.P. Negret,[5] S. Negroni,[10] T. Nunnemann,[37] D. O'Neil,[51] V. Oguri,[3] B. Olivier,[12] N. Oshima,[37] P. Padley,[62] L.J. Pan,[40] K. Papageorgiou,[28] A. Para,[37] N. Parashar,[49] R. Partridge,[59] N. Parua,[55] M. Paterno,[54] A. Patwa,[55] B. Pawlik,[22] J. Perkins,[60] M. Peters,[36] O. Peters,[20] P. Pétroff,[11] R. Piegaia,[1] H. Piekarz,[35] B.G. Pope,[51] E. Popkov,[48] H.B. Prosper,[35] S. Protopopescu,[56] J. Qian,[50] R. Raja,[37] S. Rajagopalan,[56] E. Ramberg,[37] P.A. Rapidis,[37] N.W. Reay,[45] S. Reucroft,[49] M. Ridel,[11] M. Rijssenbeek,[55] T. Rockwell,[51] M. Roco,[37]

P. Rubinov,[37] R. Ruchti,[42] J. Rutherfoord,[29] B.M. Sabirov,[23] A. Santoro,[2] L. Sawyer,[46]
R.D. Schamberger,[55] H. Schellman,[40] A. Schwartzman,[1] N. Sen,[62] E. Shabalina,[25]
R.K. Shivpuri,[16] D. Shpakov,[49] M. Shupe,[29] R.A. Sidwell,[45] V. Simak,[7] H. Singh,[34]
J.B. Singh,[15] V. Sirotenko,[37] P. Slattery,[54] E. Smith,[58] R.P. Smith,[37] R. Snihur,[40]
G.R. Snow,[52] J. Snow,[57] S. Snyder,[56] J. Solomon,[38] V. Sorín,[1] M. Sosebee,[60] N. Sotnikova,[25]
K. Soustruznik,[6] M. Souza,[2] N.R. Stanton,[45] G. Steinbrück,[53] R.W. Stephens,[60]
F. Stichelbaut,[56] D. Stoker,[33] V. Stolin,[24] A. Stone,[46] D.A. Stoyanova,[26] M. Strauss,[58]
M. Strovink,[30] L. Stutte,[37] A. Sznajder,[3] M. Talby,[10] W. Taylor,[55] S. Tentindo-Repond,[35]
S.M. Tripathi,[31] T.G. Trippe,[30] A.S. Turcot,[56] P.M. Tuts,[53] P. van Gemmeren,[37]
V. Vaniev,[26] R. Van Kooten,[41] N. Varelas,[38] L.S. Vertogradov,[23] F. Villeneuve-Seguier,[10]
A.A. Volkov,[26] A.P. Vorobiev,[26] H.D. Wahl,[35] H. Wang,[40] Z.-M. Wang,[55] J. Warchol,[42]
G. Watts,[64] M. Wayne,[42] H. Weerts,[51] A. White,[60] J.T. White,[61] D. Whiteson,[30]
J.A. Wightman,[43] D.A. Wijngaarden,[21] S. Willis,[39] S.J. Wimpenny,[34] J. Womersley,[37]
D.R. Wood,[49] R. Yamada,[37] P. Yamin,[56] T. Yasuda,[37] Y.A. Yatsunenko,[23] K. Yip,[56]
S. Youssef,[35] J. Yu,[37] Z. Yu,[40] M. Zanabria,[5] H. Zheng,[42] Z. Zhou,[43] M. Zielinski,[54]
D. Zieminska,[41] A. Zieminski,[41] V. Zutshi,[56] E.G. Zverev,[25] and A. Zylberstejn[13]

(DØ Collaboration)

[1] *Universidad de Buenos Aires, Buenos Aires, Argentina*

[2] *LAFEX, Centro Brasileiro de Pesquisas Físicas, Rio de Janeiro, Brazil*

[3] *Universidade do Estado do Rio de Janeiro, Rio de Janeiro, Brazil*

[4] *Institute of High Energy Physics, Beijing, People's Republic of China*

[5] *Universidad de los Andes, Bogotá, Colombia*

[6] *Charles University, Center for Particle Physics, Prague, Czech Republic*

[7] *Institute of Physics, Academy of Sciences, Center for Particle Physics, Prague, Czech Republic*

[8] *Universidad San Francisco de Quito, Quito, Ecuador*

[9] *Institut des Sciences Nucléaires, IN2P3-CNRS, Universite de Grenoble 1, Grenoble, France*

[10] *CPPM, IN2P3-CNRS, Université de la Méditerranée, Marseille, France*

[11] *Laboratoire de l'Accélérateur Linéaire, IN2P3-CNRS, Orsay, France*

[12] *LPNHE, Universités Paris VI and VII, IN2P3-CNRS, Paris, France*

[13] *DAPNIA/Service de Physique des Particules, CEA, Saclay, France*

[14] *Universität Mainz, Institut für Physik, Mainz, Germany*

[15] *Panjab University, Chandigarh, India*

[16] *Delhi University, Delhi, India*

[17] *Tata Institute of Fundamental Research, Mumbai, India*

[18] *Seoul National University, Seoul, Korea*

[19] *CINVESTAV, Mexico City, Mexico*

[20] *FOM-Institute NIKHEF and University of Amsterdam/NIKHEF, Amsterdam, The Netherlands*

[21] *University of Nijmegen/NIKHEF, Nijmegen, The Netherlands*

[22] *Institute of Nuclear Physics, Kraków, Poland*

[23] *Joint Institute for Nuclear Research, Dubna, Russia*

[24] *Institute for Theoretical and Experimental Physics, Moscow, Russia*

[25] *Moscow State University, Moscow, Russia*

[26] *Institute for High Energy Physics, Protvino, Russia*

[27] *Lancaster University, Lancaster, United Kingdom*

[28] *Imperial College, London, United Kingdom*

[29] *University of Arizona, Tucson, Arizona 85721*

[30] *Lawrence Berkeley National Laboratory and University of California, Berkeley, California 94720*

[31] *University of California, Davis, California 95616*

[32] *California State University, Fresno, California 93740*

[33] *University of California, Irvine, California 92697*

[34] *University of California, Riverside, California 92521*

[35] *Florida State University, Tallahassee, Florida 32306*

[36] *University of Hawaii, Honolulu, Hawaii 96822*

[37] *Fermi National Accelerator Laboratory, Batavia, Illinois 60510*

[38] *University of Illinois at Chicago, Chicago, Illinois 60607*

[39] *Northern Illinois University, DeKalb, Illinois 60115*

[40] *Northwestern University, Evanston, Illinois 60208*

[41] *Indiana University, Bloomington, Indiana 47405*

[42] *University of Notre Dame, Notre Dame, Indiana 46556*

[43] *Iowa State University, Ames, Iowa 50011*

[44] *University of Kansas, Lawrence, Kansas 66045*

[45] *Kansas State University, Manhattan, Kansas 66506*

[46] *Louisiana Tech University, Ruston, Louisiana 71272*

[47] *University of Maryland, College Park, Maryland 20742*

[48] *Boston University, Boston, Massachusetts 02215*

[49] *Northeastern University, Boston, Massachusetts 02115*

[50] *University of Michigan, Ann Arbor, Michigan 48109*

[51] *Michigan State University, East Lansing, Michigan 48824*

[52] *University of Nebraska, Lincoln, Nebraska 68588*

[53] *Columbia University, New York, New York 10027*

[54] *University of Rochester, Rochester, New York 14627*

[55] *State University of New York, Stony Brook, New York 11794*

[56] *Brookhaven National Laboratory, Upton, New York 11973*

[57] *Langston University, Langston, Oklahoma 73050*

[58] *University of Oklahoma, Norman, Oklahoma 73019*

[59] *Brown University, Providence, Rhode Island 02912*

[60] *University of Texas, Arlington, Texas 76019*

[61] *Texas A&M University, College Station, Texas 77843*

[62] *Rice University, Houston, Texas 77005*

[63] *University of Virginia, Charlottesville, Virginia 22901*

[64] *University of Washington, Seattle, Washington 98195*

(30 March 2001)

Abstract

The inclusive cross section for production of isolated photons has been measured in $p\bar{p}$ collisions at $\sqrt{s} = 630$ GeV with the DØ detector at the Fermilab Tevatron Collider. Results are presented for photons with transverse energies from 7-49 GeV and with pseudorapidity $|\eta| < 2.5$. This measurement is combined with our previous measurement at $\sqrt{s} = 1800$ GeV to form a ratio of the cross sections. Results for the 630 cross section and for the ratio are compared with next-to-leading order QCD and found to be in satisfactory agreement.
13.85.Qk, 12.38.Qk

Typeset using REVTEX

Photons produced directly from parton-parton interactions provide a powerful and effective tool for studying the constituents of hadronic matter. Because the primary production mechanism at the Tevatron is gluon Compton scattering ($qg \rightarrow \gamma q$), the cross section for direct photon production is sensitive to the gluon distribution in the proton [1]. A measurement of the final state photons provides a test of QCD without additional complications from jet identification and fragmentation.

Previous experiments, at center of mass energies of both 630 GeV [2] and 1800 GeV [3] [4], have reported photon production in excess of next-to-leading order (NLO) QCD predictions at low transverse energies ($E_T^\gamma \lesssim 30$ GeV). This larger cross section may be a result of gluon radiation not included in NLO calculations [5] or modified parton distributions [6].

In this Letter, we present a measurement of the direct, isolated photon cross section produced from $p\bar{p}$ collisions for photons with pseudorapidity in two regions, $|\eta| < 0.9$ and $1.6 < |\eta| < 2.5$ where $\eta = -\ln\tan\frac{\theta}{2}$ and θ is the angle with respect to the proton beam. We compare the production cross section at $\sqrt{s} = 630$ GeV with the previously published results at $\sqrt{s} = 1800$ GeV [3]. This comparison reduces systematic uncertainties and minimizes the sensitivity to the choice of parton distribution function.

In the simple parton model, the dimensionless cross section, $E_T^4 \cdot E\frac{d^3\sigma}{d^3p}$, as a function of $x_T = \frac{2E_T}{\sqrt{s}}$, is independent of $\sqrt{s}$. The ratio of such scaled cross sections for different energies will be unity for all values of x_T. Although deviations from this naive model are expected, the dimensionless cross section provides a useful context for comparison with QCD. This Letter presents the first measurement of the photon production cross section ratio at different center-of-mass energies using the same detector and extending η into the region greater than 1.0.

The data taken at 630 GeV and presented here represents an integrated luminosity of 520 nb^{-1} recorded in 1995 with the DØ detector at the Fermilab Tevatron [7]. The DØ detector is described in detail elsewhere [8]. The analysis uses the uranium/liquid argon calorimeter to identify photons and the drift chambers in front of the calorimeter to differentiate photon showers from electron showers. The calorimeter provides full azimuthal coverage (ϕ) and consists of a central cryostat (CC) with $|\eta| \lesssim 1.0$ and a two forward cryostats (EC) with $1.0 \lesssim |\eta| \lesssim 4.0$ each divided into four longitudinal electromagnetic layers (EM1-EM4) of 2, 2, 7, and 10 radiation lengths respectively. Layers EM1, EM2, and EM4 are transversely segmented into projective towers of angle $\Delta\phi \times \Delta\eta = 0.1 \times 0.1$ while EM3 is segmented into 0.05×0.05 sections, The electromagnetic energy resolution in the central and forward calorimeter is parameterized as $\sigma_E/E = 15\%/\sqrt{E(\mathrm{GeV})} \oplus 3\%$.

Photons interacting in the calorimeter are detected using a three-level triggering system. Level one consists of scintillation counters near the beam pipe which detect inelastic $p\bar{p}$ collisions. The second level requires a minimum energy deposition in a $\Delta\phi \times \Delta\eta = 0.2 \times 0.2$ trigger tower with trigger thresholds of 2.0, 3.0, and 7.0 GeV. In the final step, calorimeter clusters are formed with energy thresholds of 4.5, 8.0, and 14.0 GeV, respectively. The trigger efficiency for photons with energies near threshold was determined for the two highest energy triggers by taking the ratio of events passing the 14.0 (8.0) GeV trigger to those passing the 8.0 (4.5) GeV trigger in an energy regime where the lower energy trigger is 100% efficient. Monte Carlo studies of the trigger algorithms show agreement with the data for the two higher energy triggers, and were used to determine the trigger efficiency for the lowest energy trigger. Trigger efficiencies are typically about 20% at the nominal energy threshold and rise to almost 100% a few GeV above the threshold value. Consequently, photon candidates were only accepted with transverse energies of at least 7.35, 10, and 16 GeV for the three triggers, respectively.

Photon candidates were identified as energy clusters in the calorimeter. Geometric selection criteria were made to ensure that candidate photons were contained within the detector boundaries. Clusters were required to be well within the boundaries of the central calorimeter $|\eta| < 0.9$ or in the forward calorimeter $1.6 < |\eta| < 2.5$, and in the central region were required to be at least 1.6 cm from the azimuthal calorimeter section boundaries. The event vertex position was required to be within 50 cm from the nominal interaction point. The resulting geometric acceptance is $A = 0.622 \pm 0.007$ (0.787 ± 0.007) in the central (forward) region.

The photon shower was required to have a shape consistent with that of a single electromagnetic shower as determined from a calorimeter module located in a test beam of pions or electrons. The shower was required to have 96% of its energy deposited in the electromagnetic section of the calorimeter. In order to look for isolated photons, the transverse energy around the cluster had to satisfy the requirement $E_T^{\mathcal{R}\leq 0.4} - E_T^{\mathcal{R}\leq 0.2} < 2.0$ GeV where $\mathcal{R} = \sqrt{\Delta\eta^2 + \Delta\phi^2}$. The efficiency of these last three selection criteria, ϵ_s, was estimated using a detailed Monte Carlo simulation of the DØ detector. It varies as a function of E_T^γ from about 60% (75%) in the CC (EC) at 8.0 GeV, to 88% (90%) at 20 GeV and above. To reject electrons, photon candidates were rejected if any drift chamber tracks were within a road of width $\Delta\phi \times \Delta\theta = 0.2 \times 0.2$ between the initial interaction vertex and the candidate photon cluster. This selection criteria can reject actual photon candidates which converted in the material in front of the calorimeter or which have additional tracks in the road from the underlying event. This selection efficiency, as well as the efficiency for reconstructing charged tracks was estimated by studying electrons from $Z^0 \rightarrow e^+e^-$ events. The total tracking efficiency was measured to be 0.858 ± 0.013 (0.593 ± 0.079) in the central (forward) region.

The predominant remaining background comes from the decay of π^0 or η mesons to two photons. The fraction of direct photons is statistically determined from the energy (E_1) deposited deposited in the innermost longitudinal section of the calorimeter (EM1). Because neutral mesons produce two photons, the probability that at least one of them begins to shower in the calorimeter cryostat or first absorber plate is approximately twice that for a single photon. Consequently, neutral mesons tend to deposit a larger fraction of their energy in EM1 and a distribution which enhances this difference can be used to statistically determine the purity of the direct photon signal. We use the distribution of $\log_{10}[1 + \log_{10}\{1 + E_1(\mathrm{GeV})\}]$ as our discriminant.

The expected distributions from signal and background events were generated using the PYTHIA Monte Carlo [9] overlaid with minimum bias collider events to model noise and the underlying event in the detector. Fully simulated events containing photons, neutral

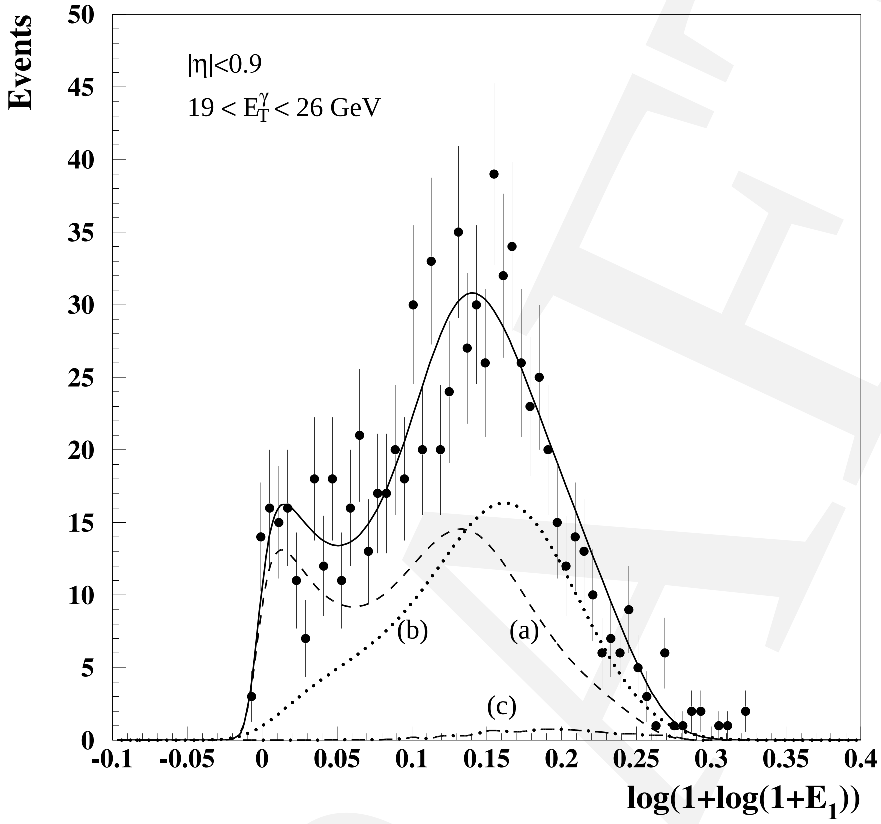

FIG. 1. Distribution of $\log_{10}[1 + \log_{10}\{1 + E_1(\mathrm{GeV})\}]$, the discriminant used for determining the purity of the final photon candidates. Points with error bars are the data. The dashed line (a) is from photons, the dotted line (b) is from neutral meson background without charged tracks and the dot-dashed line (c) is from neutral meson background with charged tracks. The sum of all three distributions is shown as the solid line.

background events, and background events with charged tracks pointing to the electromagnetic cluster were generated. The different background samples were included to minimize constraints in the purity fit from the tracking efficiency and from the model used for jet fragmentation. A systematic error due to the use of PYTHIA to model jets was estimated by varying the multiplicity of neutral mesons in the core of the jet by $\pm 10\%$. The detector response was modeled using a detailed GEANT simulation. The energy deposition response in E_1 was corrected in the Monte Carlo to match the data from $W \to e\nu$ events and from the photon data.

Identical selection criteria used to determine photon candidates in the data were applied to the Monte Carlo events. The distribution of $\log_{10}[1 + \log_{10}\{1 + E_1(\mathrm{GeV})\}]$ from the data was fit to a normalized linear combination of Monte Carlo photons plus background with and without charged tracks in the road pointing back to the interaction vertex. The fit was done as a function of E_T^γ in the central and forward rapidity regions, separately, using the fitting package HMCMLL with the fractions of signal and background constrained to be between 0.0 and 1.0 [10]. The purity ($\mathcal{P}$), is defined as the fraction of Monte Carlo photons in the normalized fit distribution. A representative fit is shown in Fig. 1 and the photon purity as a function of E_T^γ is plotted in Fig. 2.

After applying efficiency and purity corrections, the final cross section $d^2\sigma/dE_T^\gamma d\eta$ is calculated. The results are shown in Fig. 3 and tabulated in Table I. The error bars show all uncorrelated uncertainties which include the statistical uncertainty, the purity fitting error, and the uncertainty on the selection criteria and the trigger efficiency. The contribution from the purity fit is the largest source of uncorrelated uncertainty. The correlated uncertainty consists of the uncertainty on the luminosity, the tracking efficiency, the geometric acceptance, the calorimeter energy scale, and the largest contribution from the fragmentation model.

The results are compared with NLO QCD calculations using CTEQ4M as implemented by Baer, Ohnemus, and Owens [11] and, in the central region, CTEQ5M as implemented by Vogelsang [12]. Renormalization and factorization scales of $\mu_R = \mu_F = E_T^{\max}$ where

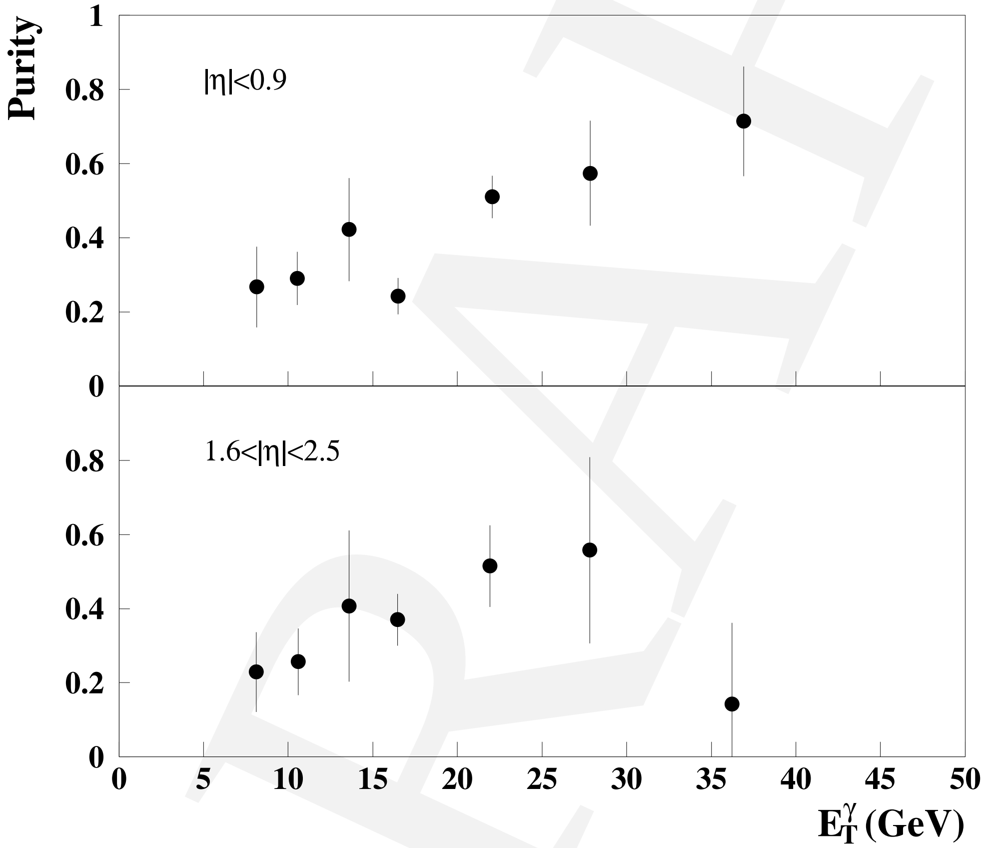

FIG. 2. The photon purity as a function of E_T^γ for central and forward photons.

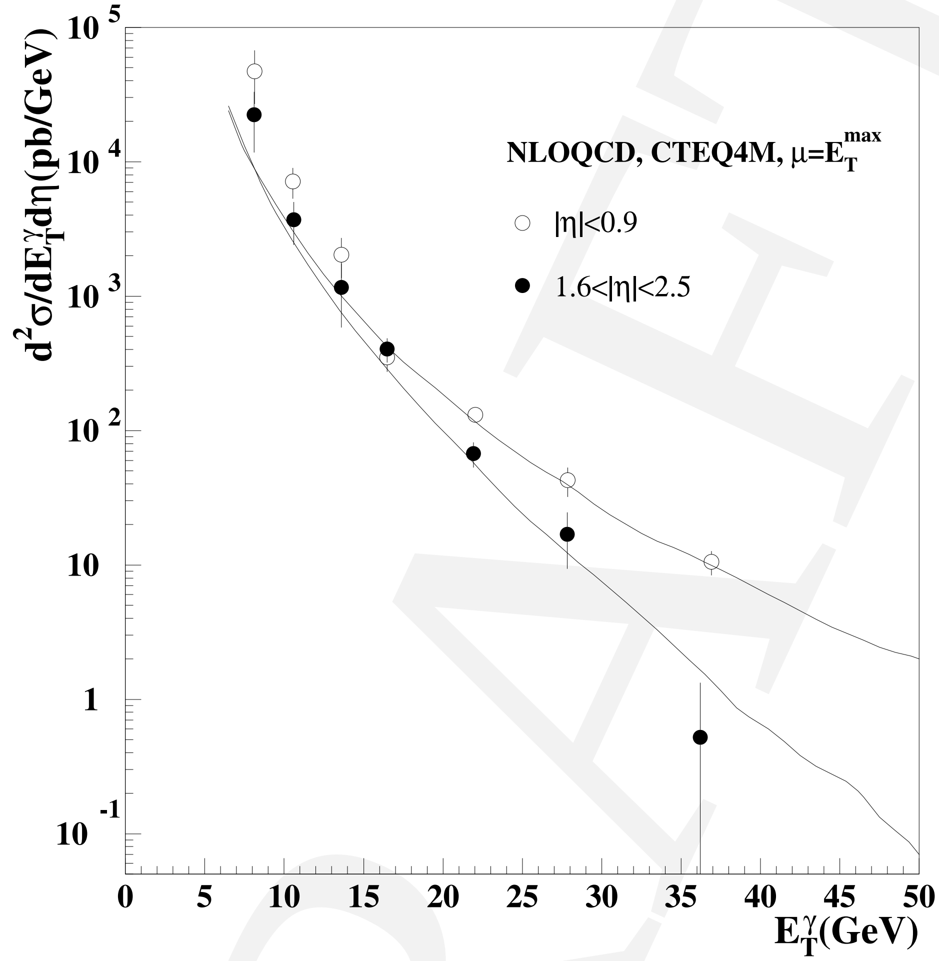

FIG. 3. The cross section for production of isolated photons in the central and forward regions. The error bars show the complete uncorrelated error and the curves show NLO QCD calculated cross sections.

E_T^γ Range (GeV)	Fit E_T^γ (GeV)	$d\sigma/dE_T^\gamma d\eta$ NLO QCD	(pb/GeV) measured	$\delta\sigma_U$ (%)	$\delta\sigma_C$ (%)
		$\lvert\eta\rvert < 0.9$			
7.35- 9.1	8.2	8220	47000	43	52
9.1-12.6	10.5	2960	7160	26	36
12.6-14.7	13.6	1022	2040	33	25
14.7-18.9	16.5	416	351	22	19
18.9-26.25	22.1	117	131	11	13
26.25-29.75	27.9	37.1	42.6	25	10
29.75-49.0	36.9	9.18	10.5	21	7
		$1.6 < \lvert\eta\rvert < 2.5$			
7.35- 9.1	8.1	8470	22400	48	42
9.1-12.6	10.6	2500	3700	35	31
12.6-14.7	13.6	766	1170	50	24
14.7-18.9	16.5	283	403	20	21
18.9-26.3	21.9	56.9	67.3	22	17
26.25-29.75	27.8	11.2	16.9	45	16
29.75-49.0	36.2	1.86	.522	160	15

TABLE I. The measured and predicted isolated photon production cross section. The column labeled Fit E_T^γ is the energy where a fit to the falling production cross section has the same value as that measured, and is approximately equal to the average value of $\langle E_T \rangle$ and $E_T^{(\mathrm{mid})}$ where $\langle E_T \rangle$ is the average energy in each bin and E_T^{mid} is the mid-point energy in each bin. The columns labeled δ_U and δ_C are the uncorrelated and correlated uncertainties, respectively.

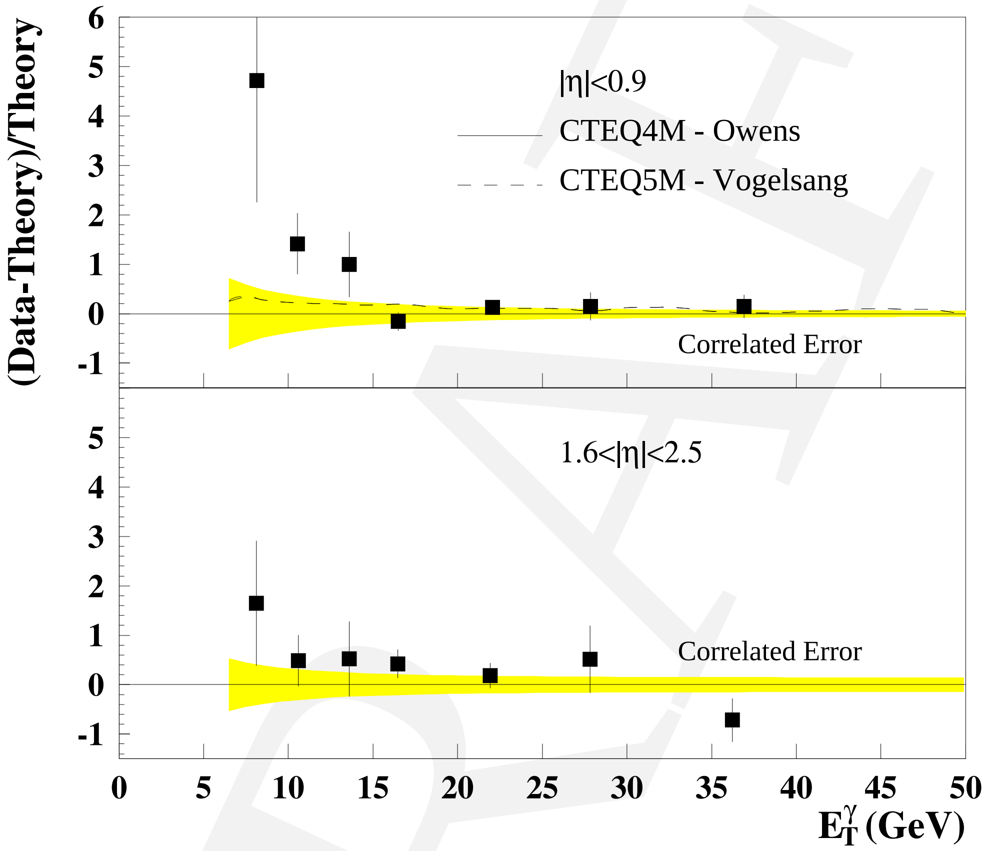

FIG. 4. Comparison of the measured cross section for production of isolated photons to the prediction of NLO QCD using CTEQ4M and CTEQ5M parton distribution functions.

used. Owens *et.al.* define $E_T^{\max}$ as the larger of the transverse energies of the photon or leading jet and Vogelsang defines $E_T^{\max}$ as the largest photon transverse energy. Fig. 4 shows the comparison between the data and theory normalized to the theory. A covariance matrix χ^2 provides a measure of the probability that the theory describes the measured data. A complete covariance matrix comprised of correlated and uncorrelated uncertainties was determined and the data was fit to the theoretical cross section with a χ^2 value of 11.6 (6.76) for 7 degrees of freedom in the CC (EC). This gives a standard χ^2 probability that the data fits the theory of 11.5% (45.4%) in the CC (EC).

We combine the cross section measured in this Letter with that measured at 1800 GeV and reported in Ref. [3]. The cross section at 1800 GeV has been increased in every bin by 3.4% from the published result due to recent measurements of the proton-antiproton total cross section [13]. The experimental dimensionless cross section, averaged over azimuth, is given by $\frac{E_T^3}{2\pi} \cdot d^2\sigma/dE_T d\eta$. The ratio of the dimensionless cross sections ($\sqrt{s} = 630$ GeV/$\sqrt{s} =$ 1800 GeV) is shown in Fig. 5 as a function x_T.

The uncorrelated uncertainty comes from the purity fit, the selection efficiency, the trigger efficiency, the longitudinal vertex requirement, and the energy scale correction. The correlated uncertainty has contributions from the fragmentation model, the determination of the luminosity, the geometric acceptance, and the tracking efficiency. The results of the ratio measurement are shown in Table II.

A comparison between the measured ratio and that from the NLO QCD calculation is made by determining a χ^2 value that the data matches the theory using the complete covariance matrix. The data was fit to the theoretical cross section with a χ^2 value of 6.45 (4.26) for 7 degrees of freedom in the CC (EC). This gives a standard χ^2 probability that the data fits the theory of 48.8% (74.9%) in the CC (EC). Although the lowest x_T points are systematically higher than NLO QCD predictions in both the EC and the CC, the overall results indicate good agreement between the measured ratio and the theory.

In conclusion, we have measured the production cross section for isolated photons in $p\overline{p}$ collisions at $\sqrt{s} = 630$ GeV and compared this cross section with that measured at

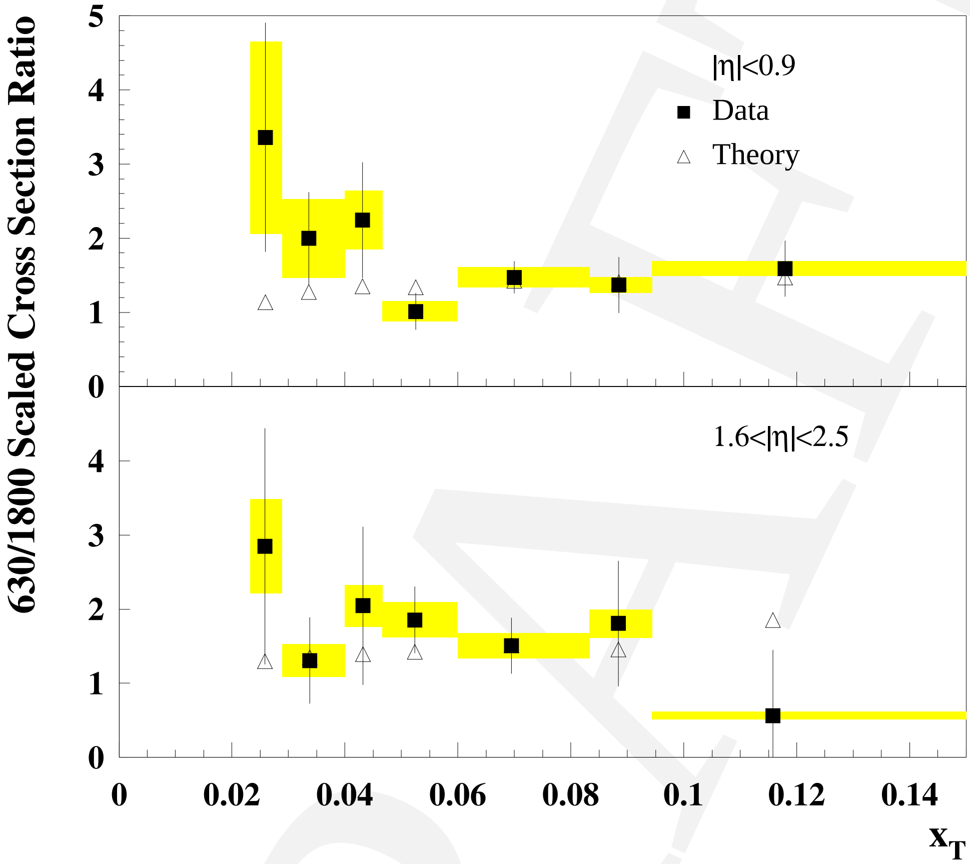

FIG. 5. The ratio of the dimensionless cross section $(\frac{E_T^3}{2\pi} \cdot d^2\sigma/dE_T d\eta)$ for $\sqrt{s}$ = 630 GeV/$\sqrt{s}$ = 1800 GeV. The error bars show the uncorrelated uncertainty and the shaded bands show the correlated contribution to the diagonal terms of the covariance matrix.

x_T Range	Fit x_T	Ratio	Theory	$\delta\sigma_U(\%)$	$\delta\sigma_C$ (%)
		$\lvert\eta\rvert < 0.9$			
0.023-0.029	0.026	3.36	1.13	46	39
0.029-0.040	0.034	2.00	1.27	31	27
0.040-0.047	0.043	2.24	1.34	34	18
0.047-0.060	0.053	1.01	1.34	25	13
0.060-0.083	0.070	1.46	1.43	15	9
0.083-0.094	0.089	1.37	1.41	28	8
0.094-0.156	0.118	1.59	1.47	24	7
		$1.6 < \lvert\eta\rvert < 2.5$			
0.023-0.029	0.026	2.84	1.30	56	22
0.029-0.040	0.034	1.31	1.35	45	17
0.040-0.047	0.043	2.05	1.39	52	14
0.047-0.060	0.052	1.86	1.42	24	13
0.060-0.083	0.070	1.51	1.52	25	11
0.083-0.094	0.088	1.81	1.46	47	11
0.094-0.156	0.116	0.563	1.86	160	10

TABLE II. The measured ratio (Ratio) and NLO QCD prediction (Theory) for the dimensionless cross section at $\sqrt{s} = 630$ GeV to that at $\sqrt{s} = 1800$ GeV. The columns labeled δ_U and δ_C are the uncorrelated and correlated uncertainties, respectively.

$\sqrt{s} = 1800$ GeV. Although some discrepancies exist between the measurement and NLO QCD at the lowest E_T bins in both the cross section measurement and the ratio, there is good agreement between the data and the theoretical prediction.

We thank J.F. Owens and W. Vogelsang for their assistance with the theoretical calculations. We thank the staffs at Fermilab and collaborating institutions, and acknowledge support from the Department of Energy and National Science Foundation (USA), Commissariat à L'Energie Atomique and CNRS/Institut National de Physique Nucléaire et de Physique des Particules (France), Ministry for Science and Technology and Ministry for Atomic Energy (Russia), CAPES and CNPq (Brazil), Departments of Atomic Energy and Science and Education (India), Colciencias (Colombia), CONACyT (Mexico), Ministry of Education and KOSEF (Korea), CONICET and UBACyT (Argentina), The Foundation for Fundamental Research on Matter (The Netherlands), PPARC (United Kingdom), Ministry of Education (Czech Republic), and the A.P. Sloan Foundation.

REFERENCES

[1] Owens, J., Rev. Mod. Phys. **59** 465 (1987).

[2] UA2 Collaboration, J. Attili *et.al.*, Phys. Rev. **B263** (1991) 544; UA2 Collaboration, R. Ansari *et.al.*, Z. Phys. C **41** 395 (1988).

[3] DØ Collaboration, B. Abbott *et.al.*, Phys. Rev. Lett. **84** 2786 (2000).

[4] CDF Collaboration, F. Abe *et.al.*, Phys. Rev. Lett. **73** 2662 (1994), CDF Collaboration, F. Abe *et.al.*, Phys. Rev. D **48** 2998 (1993).

[5] J. Huston *et.al.*, Phys. Rev. D **51** 6139 (1995), H.-L. Lai and H.-N. Li, Phys. Rev. D **58** 114020 (1998), L. Apanasevich *et.al.*, Phys. Rev. D **59** 074007 (1999).

[6] M. Glück, *et.al.*, Phys. Rev. Lett. **73** 388 (1994), W. Vogelsang and A. Vogt, Nucl. Phys. **B453**, 334 (1995a).

[7] J. Krane, J. Bantley, and D. Owen, Fermilab-TM-2000, 1997, (unpublished).

[8] DØ Collaboration, S. Abachi *et.al.*, Nucl. Instr. Meth. **A338** 185 (1994).

[9] T. Sjöstrand, Comput. Phys Commun.**82** 74 (1995).

[10] R. Barlow and C. Beeston, Comput. Phys. Commun. **77** 219 (1993).

[11] H.Baer, J. Ohnemus, J.F. Owens, Phys. Rev, **D42** 61 (1990).

[12] W. Vogelsang and A. Vogt, Nucl. Phys. **B453** 334 (1995).

[13] E811 Collaboration, C. Avila *et.al.*, Phys. Lett.**B445** 419 (1999); DØ Collaboration, B. Abbott *et.al.*, Phys. Rev. **D61** 072001 (2000).